Journal of Hydroscience and Hydraulic Engineering
Vol. 10, No. 2, November, 1992, 51-60

NUMERICAL SIMULATION OF EUTROPHICATION PHENOMENA IN A RESERVOIR BY MEANS OF PLANE MULTI-LAYERED MODEL

By

Naoki Matsuo

Department of Civil Engineering, Chubu University, Aichi, Japan

Yoshiaki Iwasa

Department of Civil Engineering, Kyoto University, Kyoto, Japan

Sukeaki Shiino

Yonden Engineering Consultants Corporation, Takamatsu, Japan

and

Tetsuya Yamada

Public Works Research Institute, Ministry of Construction, Tsukuba, Japan

SYNOPSIS

This paper deals with the numerical simulation of eutrophication phenomena coupled with hydrodynamic behaviours of stored water in a stratified reservoir. A plane multi-layered simulation model is deduced from the hydrodynamic principles in the curvilinear orthgonal coordinate system which is favourable to the realization of geometrical features considered in this study. The phytoplankton blooming in the Muroh Reservoir is simulated and the results are discussed to illustrate the validity of the proposed model.

INTRODUCTION

The eutrophication phenomena in many reservoirs are characterized by often localized phytoplankton blooms. They are strongly influenced by hydrodynamics of stored water which in turn is affected by reservoir shape and boundary conditions of flows(5). The aim of study is to disclose the relation between characteristics of reservoir hydrodynamics and kinetic changes of water quality parameters concerning the phytoplankton blooms. This is important to evaluate the essential features of eutrophication phenomena and establish the effective technique of rehabilitation in deteriorated reservoirs.

For the purpose of present aim, the dynamics of physical, chemical and biological factors relating phytoplankton production must be analized in a three-dimensional view of the phenomena. In lakes, such analyses have been made by plane multi-layered models which are usually developed in the Cartesian coordinate system(4).

In this study, a plane multi-layered model(6) is developed in the curvilinear orthogonal coordinate system. The model incorporates the geometrical feature in deep reservoirs with complicated boundaries(2). This numerical simulation model fits the spatial uniformity of the phenomena and will be able to realize the hydraulic behaviours of stored water responding to the complicated boundary conditions in reservoirs. The present case study is carried out for the Muroh Reservoir and the process of algae blooming after a flood inflow with a large amount of nutrients is simulated.

NUMERICAL SIMULATION MODELS

Mathematical model of simulation study

Many of reservoirs in Japan belong to deep gorge type along the rivers of snaky curves. In such reservoirs, the uni-directional flow along the channel is dominant. Furthermore, the dynamical change of flow is usually very slow. The Boussinesq's approximation and the hydrostatic pressure distribution in the vertical direction are applied to the flow dynamics.

Curvilinear orthogonal coordinate system is used to develop the simulation model in order to better represent the geometrical and hydrodynamic characteristics of the reservoir. In this coordinate system, x_1 and x_2 axes alined on the horizontal plane and x_3 axis is on the vertical one.

The basic mathematical model is derived from the hydrodynamic principles. The mathematical model consists of the continuity equation, two components of the momentum conservation law on the horizontal plane, the hydrostatic law in the vertical direction, the heat balance equation of the water temperature and the concentration balance equation of water quality parameters. These equations are averaged after making integration with respect to the control volumes illustrated in Fig.1. The basic model is then transformed into the plane multi-layered model. In this study, x_1 axis is aligned in the longitudinal direction along the channel and x_2 axis is in the transverce direction which make a right angle with x_1 as shown in Fig.1. Furthermore, two transformation coefficients, h_2 in the x_2-direction and h_3 in the x_3-direction, are set to 1.0.

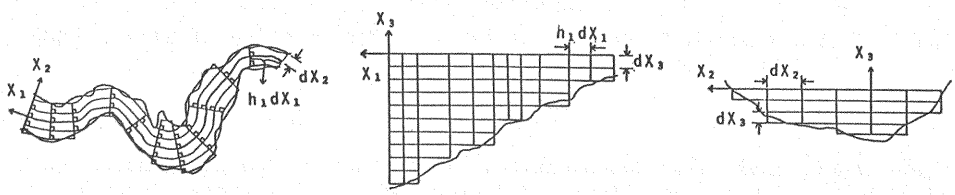

horizontal plane longitudinal section transverse section

Fig. 1 Coordinate system and control volume used in the simulation

The governing equations describing for the inner blocks are as follows:

(1) continuity equation;

$$\frac{1}{h_1 dx_1} \left| u_1 \right|_{x_{1i}}^{x_{1i+1}} + \frac{1}{h_1 dx_2} \left| h_1 u_2 \right|_{x_{2j}}^{x_{2j+1}} + \frac{1}{dx_3} \left| u_3 \right|_{x_{3k}}^{x_{3k+1}} = 0 \tag{1}$$

(2) x_1-direction component of momentum conservation law;

$$\begin{aligned} &\frac{\partial u_1}{\partial t} + \frac{1}{h_1 dx_1} \left| u_1 u_1 \right|_{x_{1i}}^{x_{1i+1}} + \frac{1}{h_1 dx_2} \left| h_1 u_2 u_1 \right|_{x_{2j}}^{x_{2j+1}} + \frac{1}{dx_3} \left| u_3 u_1 \right|_{x_{3k}}^{x_{3k+1}} \\ &= -\frac{1}{\rho h_1 dx_1} \left| p \right|_{x_{1i}}^{x_{1i+1}} + \frac{1}{h_1 dx_1} \left| \frac{E_{x_1 x_1}}{h_1} \left(\frac{\partial u_1}{\partial x_1} + u_2 \frac{\partial h_1}{\partial x_2} \right) \right|_{x_{1i}}^{x_{1i+1}} \\ &+ \frac{1}{h_1 dx_2} \left| E_{x_1 x_2} h_1^2 \frac{\partial}{\partial x_2} \left(\frac{u_1}{h_1} \right) \right|_{x_{2j}}^{x_{2j+1}} + \frac{1}{dx_3} \left| E_{x_1 x_3} \frac{\partial u_1}{\partial x_3} \right|_{x_{3k}}^{x_{3k+1}} \\ &+ \frac{1}{h_1 dx_2} \left[E_{x_1 x_2} \left(\frac{1}{h_1} \frac{\partial u_2}{\partial x_1} + h_1 \frac{\partial}{\partial x_2} \left(\frac{u_1}{h_1} \right) \right) - u_1 u_2 \right] \left| h_1 \right|_{x_{2j}}^{x_{2j+1}} \end{aligned} \tag{2}$$

(3) x_2-direction component of momentum conservation law;

$$\begin{aligned} &\frac{\partial u_2}{\partial t} + \frac{1}{h_1 dx_1} \left| u_1 u_2 \right|_{x_{1i}}^{x_{1i+1}} + \frac{1}{h_1 dx_2} \left| h_1 u_2 u_2 \right|_{x_{2j}}^{x_{2j+1}} + \frac{1}{dx_3} \left| u_3 u_2 \right|_{x_{3k}}^{x_{3k+1}} \\ &= -\frac{1}{\rho dx_2} \left| p \right|_{x_{2j}}^{x_{2j+1}} + \frac{1}{h_1 dx_1} \left| \frac{E_{x_1 x_2}}{h_1} \frac{\partial u_2}{\partial x_1} \right|_{x_{1i}}^{x_{1i+1}} \\ &+ \frac{1}{h_1 dx_2} \left| E_{x_2 x_2} h_1 \frac{\partial u_2}{\partial x_2} \right|_{x_{2j}}^{x_{2j+1}} + \frac{1}{dx_3} \left| E_{x_2 x_3} \frac{\partial u_2}{\partial x_3} \right|_{x_{3k}}^{x_{3k+1}} \end{aligned}$$

$$-\frac{1}{h_1 dx_2}\left(\frac{E_{x_1x_1}}{h_1}\left(\frac{\partial u_1}{\partial x_1}+u_2\frac{\partial h_1}{\partial x_2}\right)-u_1u_1\right)\mid h_1\mid_{x_{2j}}^{x_{2j+1}} \tag{3}$$

(4) x_3-direction component of momentum conservation law (hydrostatic law);

$$p=\int_{x_3}^{x_{3s}}\rho g\,dx_3 \tag{4}$$

(5) heat balance equation of water temperature;

$$\begin{aligned}\frac{\partial T}{\partial t}&+\frac{1}{h_1dx_1}\mid u_1T\mid_{x_{1i}}^{x_{1i+1}}+\frac{1}{h_1dx_2}\mid h_1u_2T\mid_{x_{2j}}^{x_{2j+1}}+\frac{1}{dx_3}\mid u_3T\mid_{x_{3k}}^{x_{3k+1}}\\&=\frac{1}{h_1dx_1}\mid\frac{D_{Tx_1}}{h_1}\frac{\partial T}{\partial x_1}\mid_{x_{1i}}^{x_{1i+1}}+\frac{1}{h_1dx_2}\mid D_{Tx_2}h_1\frac{\partial T}{\partial x_2}\mid_{x_{2j}}^{x_{2j+1}}\\&+\frac{1}{dx_3}\mid D_{Tx_3}\frac{\partial T}{\partial x_3}\mid_{x_{3k}}^{x_{3k+1}}+H_T\end{aligned} \tag{5}$$

(6) concentration balance equation of water quality parameters;

$$\begin{aligned}\frac{\partial c}{\partial t}&+\frac{1}{h_1dx_1}\mid u_1c\mid_{x_{1i}}^{x_{1i+1}}+\frac{1}{h_1dx_2}\mid h_1u_2c\mid_{x_{2j}}^{x_{2j+1}}+\frac{1}{dx_3}\mid u_3c\mid_{x_{3k}}^{x_{3k+1}}\\&=\frac{1}{h_1dx_1}\mid\frac{D_{cx_1}}{h_1}\frac{\partial c}{\partial x_1}\mid_{x_{1i}}^{x_{1i+1}}+\frac{1}{h_1dx_2}\mid D_{cx_2}h_1\frac{\partial c}{\partial x_2}\mid_{x_{2j}}^{x_{2j+1}}\\&+\frac{1}{dx_3}\mid D_{cx_3}\frac{\partial c}{\partial x_3}\mid_{x_{3k}}^{x_{3k+1}}+S_c+P_c\end{aligned} \tag{6}$$

For the blocks lying on particular boundaries, Eqs.1 to 6 are transformed to incorporate the geometric and kinetic conditions at the boundaries.

Water quality model of eutrophication phenomena

The main parameter of water quality in the present study is chlorophyl-a content of three species of phytoplankton, i.e. blue-green algae, green algae and diatoms(1). The other parameters are carbon in zooplankton, inorganic and organic nitrogens, inorganic and organic phosphorus and chemical oxygen demand. In modelling ecological processes, growth, respiration and grazing of phytoplankton, growth and mortality of zooplankton, algal uptake, minaralization and zooplankton's excretion of nutrients, and production and decomposition of chemical oxygen demand are taken into consideration. Their kinetics are represented mathematically under the following assumptions.

a) Temperature dependency of the kinetic change on the ecological processes is represented by an exponential function of water temperature. As to the primary production of the phytoplanktons, inhibition of high temperature above a certain level is introduced(7).

b) Effect of the light intensity on the primary production is also represented by an exponential function of solar radiation with inhibition of the irradiation above a certain level.

c) Effect of the nutrient concentrations on the primary production and of saturation on the grazing rate are represented by Monod's function.

d) Spatial effect on the primary production is expressed by an exponential function of the chlorophyl-a concentration.

The concentration balance equations of water quality parameters are as follows:

(1) balance equation of chlorophyl-a in phytoplanktons

(i=1:diatoms, i=2:green algae, i=3:blue-green algae)

$$\frac{\partial C_{P_i}}{\partial t}=F(C_{P_i})-\frac{1}{dx_3}\mid C_{P_i}\cdot w_{C_{P_i}}\mid_{x_{3k}}^{x_{3k+1}}+G_{C_{P_i}}-R_{C_{P_i}}\theta_{C_{P_i}}^{(T-20)}C_{P_i}-G_{z_i} \tag{7}$$

(2) balance equation of carbon in zooplankton

$$\frac{\partial Z}{\partial t} = F(Z) + \sum_i \alpha_i a_{z_i} G_{z_i} - R_z \theta_z^{(T-20)} Z \tag{8}$$

(3) balance equation of inorganic nitrogen

$$\frac{\partial N_I}{\partial t} = F(N_I) - \sum_i \beta_N G_{C_{P_i}} + R_N \theta_N^{(T-20)} (N_O - \sum_i \beta_N C_{P_i} - \gamma_N Z) + \sum_i \beta_N (1 - a_{z_i}) G_{z_i} \tag{9}$$

(4) balance equation of organic nitrogen

$$\frac{\partial N_O}{\partial t} = F(N_O) - \frac{1}{dx_3} \mid (N_O - \gamma_N Z) \cdot w_{N_O} \mid_{x_{3k}}^{x_{3k+1}} + \sum_i \beta_N G_{C_{P_i}} - R_N \theta_N^{(T-20)} (N_O - \sum_i \beta_N C_{P_i} - \gamma_N Z) - \sum_i \beta_N (1 - a_{z_i}) G_{z_i} \tag{10}$$

(5) balance equation of inorganic phosphorus

$$\frac{\partial P_I}{\partial t} = F(P_I) - \sum_i \beta_P G_{C_{P_i}} + R_P \theta_P^{(T-20)} (P_O - \sum_i \beta_P C_{P_i} - \gamma_P Z) + \sum_i \beta_P (1 - a_{z_i}) G_{z_i} \tag{11}$$

(6) balance equation of organic phosphorus

$$\frac{\partial P_O}{\partial t} = F(P_O) - \frac{1}{dx_3} \mid (P_O - \gamma_P Z) \cdot w_{P_O} \mid_{x_{3k}}^{x_{3k+1}} + \sum_i \beta_P G_{C_{P_i}} - R_P \theta_P^{(T-20)} (P_O - \sum_i \beta_P C_{P_i} - \gamma_P Z) - \sum_i \beta_P (1 - a_{z_i}) G_{z_i} \tag{12}$$

(7) balance equation of chemical oxygen demand

$$\frac{\partial C_O}{\partial t} = F(C_O) - \frac{1}{dx_3} \mid C_O \cdot w_{C_O} \mid_{x_{3k}}^{x_{3k+1}} + f_P G_{C_P} - f_C C_O \tag{13}$$

where

$$G_{C_{P_i}} = S_{P_i} \cdot R_{G_i} \{ \frac{T}{T_{f_i}} \cdot \exp\left(1 - \frac{T}{T_{f_i}}\right) \}^{ni} \cdot \frac{I_{x_3}}{I_{S_i}} \exp\left(1 - \frac{I_{x_3}}{I_{s_i}}\right) \cdot \frac{N_I}{K_{N_I} + N_I} \cdot \frac{P_I}{K_{P_I} + P_I}$$

$$S_{P_i} = \exp(-\mu_s C_{P_i})$$

$$I_{x_3} = I_O \cdot \exp\{-\eta (x_{3S} - x_3)\}$$

$$\eta = \eta_0 + \mu_n \sum_i C_{P_i}$$

$$G_{z_i} = d_i \frac{K_{C_{P_i}}}{K_{C_{P_i}} + C_{P_i}} \cdot C_{P_i} \cdot Z$$

The first terms on the right hand side of Eqs.7 to 13 indicate convection and dispersion of the water qualty parameters. Their expression is as follows:

$$F(c_j) = -\frac{1}{h_1 h_2 dx_1} \mid h_2 u_1 c_j \mid_{x_{1i}}^{x_{1i+1}} - \frac{1}{h_1 h_2 dx_2} \mid h_1 u_2 c_j \mid_{x_{2j}}^{x_{2j+1}} - \frac{1}{dx_3} \mid u_3 c_j \mid_{x_{3k}}^{x_{3k+1}} + \frac{1}{h_1 h_2 dx_1} \mid \frac{D_{cx_1} h_2}{h_1} \frac{\partial c_j}{\partial x_1} \mid_{x_{1i}}^{x_{1i+1}} + \frac{1}{h_1 h_2 dx_2} \mid \frac{D_{cx_2} h_1}{h_2} \frac{\partial c_j}{\partial x_2} \mid_{x_{2j}}^{x_{2j+1}} + \frac{1}{dx_3} \mid D_{cx_3} \frac{\partial c_j}{\partial x_3} \mid_{x_{3k}}^{x_{3k+1}} \qquad (c_j = C_{p_i}, Z, N_I, N_O, P_I, P_O, C_O \quad) \tag{14}$$

The second terms in Eqs.7, 10, 12 and 13 represent settling of phytoplankton and undissolved nutrients.

NUMERICAL SIMULATION AND DISCUSSION

Numerical simulation

The plane multi-layered model is applied to simulate eutrophication phenomena in the Muroh Reservoir. The Muroh Reservoir is a multi-purpose reservoir located in Nara Prefecture. The outline of the reservoir is as follows: the dam height = 63.5m , capacity = $16.9 \times 10^6 m^3$, water surface area = $1.05 km^2$, length =5.8km, and elevation of outlet for flood = 282m. The intake at the dam is operated to keep 3m depth from the water surface. Another intake for water supply is located at 2.4km upstream from the dam. The reservoir is thermally stratified in warm seasons.

The hydrodynamics of the stored water and the changes of water quality parameters are computed using hydrodynamic and meteorological observations during 24 days from 15 August to 7 September in 1983. The staggered scheme, which is a kind of explicit finite difference method, is used in the numerical computation. For the spatial derivatives, the upwind difference for convection terms and the central difference for dispersion terms are used. For the time derivatives, the balance equations of water quality parameters are developed by the two-step Runge-Kutter scheme to avoid unstableness in solution due to non-linear reaction terms.

Initial and boundary conditions used in the computation are as follows:

1) Initial condition; The distribution of velocities is estimated under the steady state condition of flow at initial time. The observed data are used for the temperature and the concentration of water quality parameters.

2) Boundary condition; The fluxes of all variables across the solid boundary are assumed to be zero and the non-slip condition of flow is specified at the boundary. The meteorological heat exchanges are considered at the water surface.

Spatial grid used in the simulation must be determined to suit the scales of the phenomena(3). The water body is divided into the blocks utilizing the survey data at intervals of 200m in the flow direction. The thickness and the width of each block are fixed to be 2m and 30m, respectively. The time step is determined to satisfy the stability condition of the numerical solution. The time step of 1.5 seconds for the flow and 300 seconds for the water quality parameters are used.

Simulation results and discussion

The computed results are shown in Fig.2 to Fig.5. Fig.2 shows the distributions of flow velocity in the surface layer(EL.283m), the upper layer(EL.279m) and the middle layer(EL.275m). The elevation values indicate center heights of the layers except for the surface layer. In the surface layer, the block thicknesses are estimated by the continuity equation. The characteristics of flow patterns are recognized in Fig.2 as follows:

1) On 15 August before a flood will come, the discharge from the intake at Hatsuse (QOUT1 in Fig.2), which is located at 2.4km upstream from the dam and at 275m in height above the sea level, is larger than that from the outlet work (QOUT2 in Fig.2). Therefore, the flow towards the intake is relatively dominant except for the flow in the surface layer which is strongly affected by the discharge from the outlet. The flow at this time is very slow and the flow velocities are almost less than 1m/min in each layer.

2) On 16 August when a flood passes into the reservoir, a greater part of the stored water flows downstream towards the outlet (QOUT3 in Fig.2) with the velocities of 1 to 20 m/min. Influence of the intake at Hatsuse is no longer significant at this time.

3) After the flood passed, the flow conditions return again to the previous one. The result on 24 August shows that the inflow water plunges into the layer of 7m to 8m in depth because its temperature is lower than the stored water. The plunging flow, which travells downstream, branches off into two parts with the circulation in the lateral direction at 1km upstream from the dam body. One part of the branched flow travells upstream in the surface layer and the other travells downstream. The

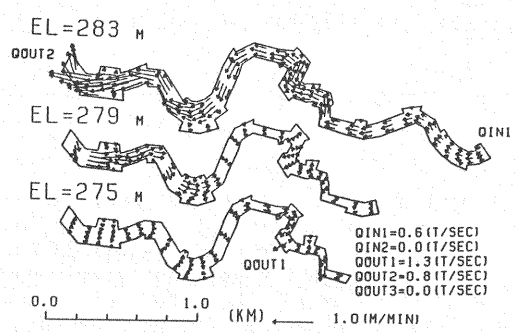

(a) 15 August

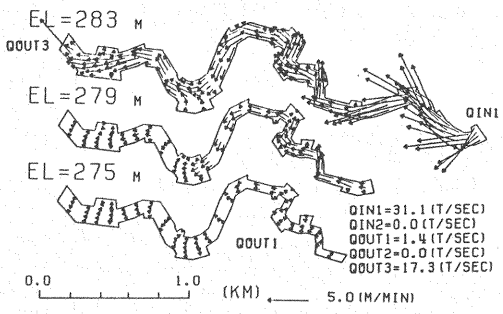

(b) 16 August

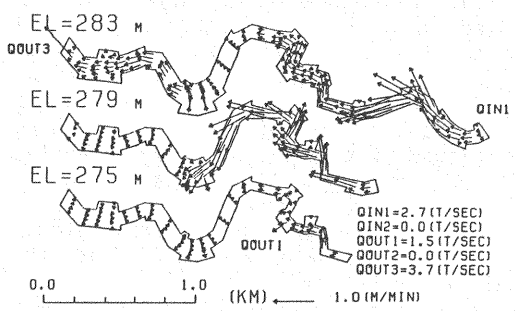

(c) 24 August

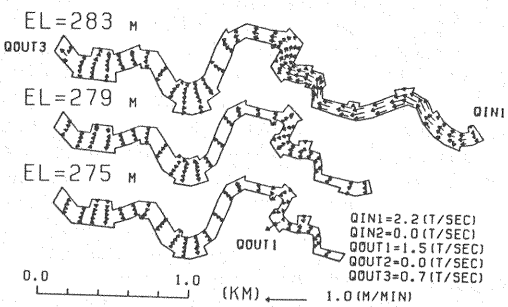

(d) 31 August

Fig.2 Simulated distributions of flow velocity

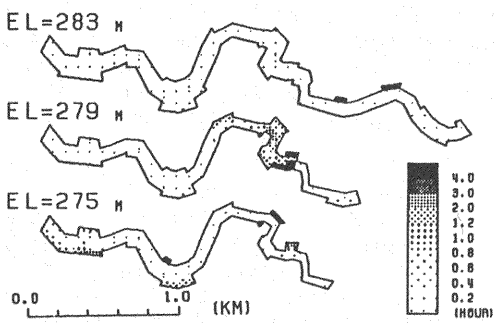

(a) 15 August

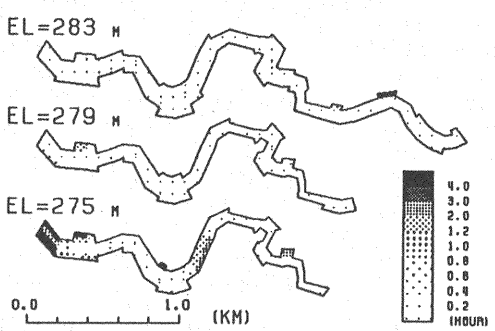

(b) 16 August

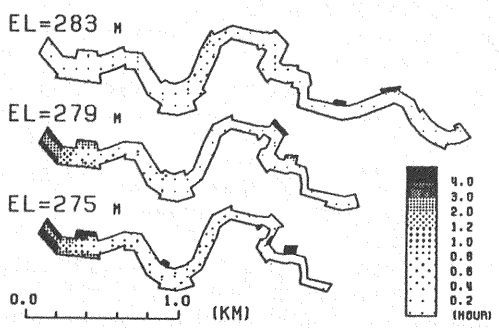

(c) 24 August

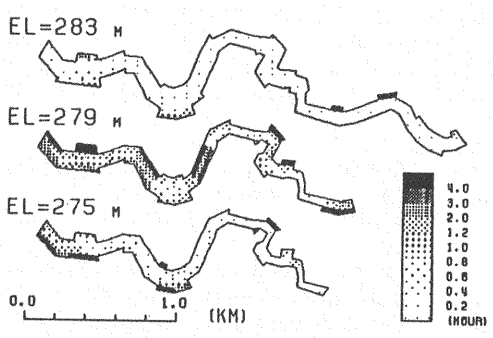

(d) 31 August

Fig.3 Simulated distributions of retention time

plunging of inflow water including flood flows usually occurs at the point where the slope of the channel becomes steeper suddenly. This indicates that the shape of the longitudinal section of the reservoir influences significantly on the plunging point.

Fig.3 shows the retention time of flow computed for the unit volume ($1m^3$), and their characteristics are recognized as follows:

1) Under calm flow conditions as seen in Fig.3(a),(c) and (d), the distributions of retention time in the surface layer remain the same. The retentive area does not exist except for the inlets.

2) The influence of the dam body at the downstream end and that of the intake at Hatsuse are notable in the upper and middle layers. For example, the results on 15 August shows that the retentive area in the upper layer is formed in the vicinity of the intake where the flow is stagnant between the downstream surface flow and the upstream middle one. Long retentive areas are also seen between the intake and the

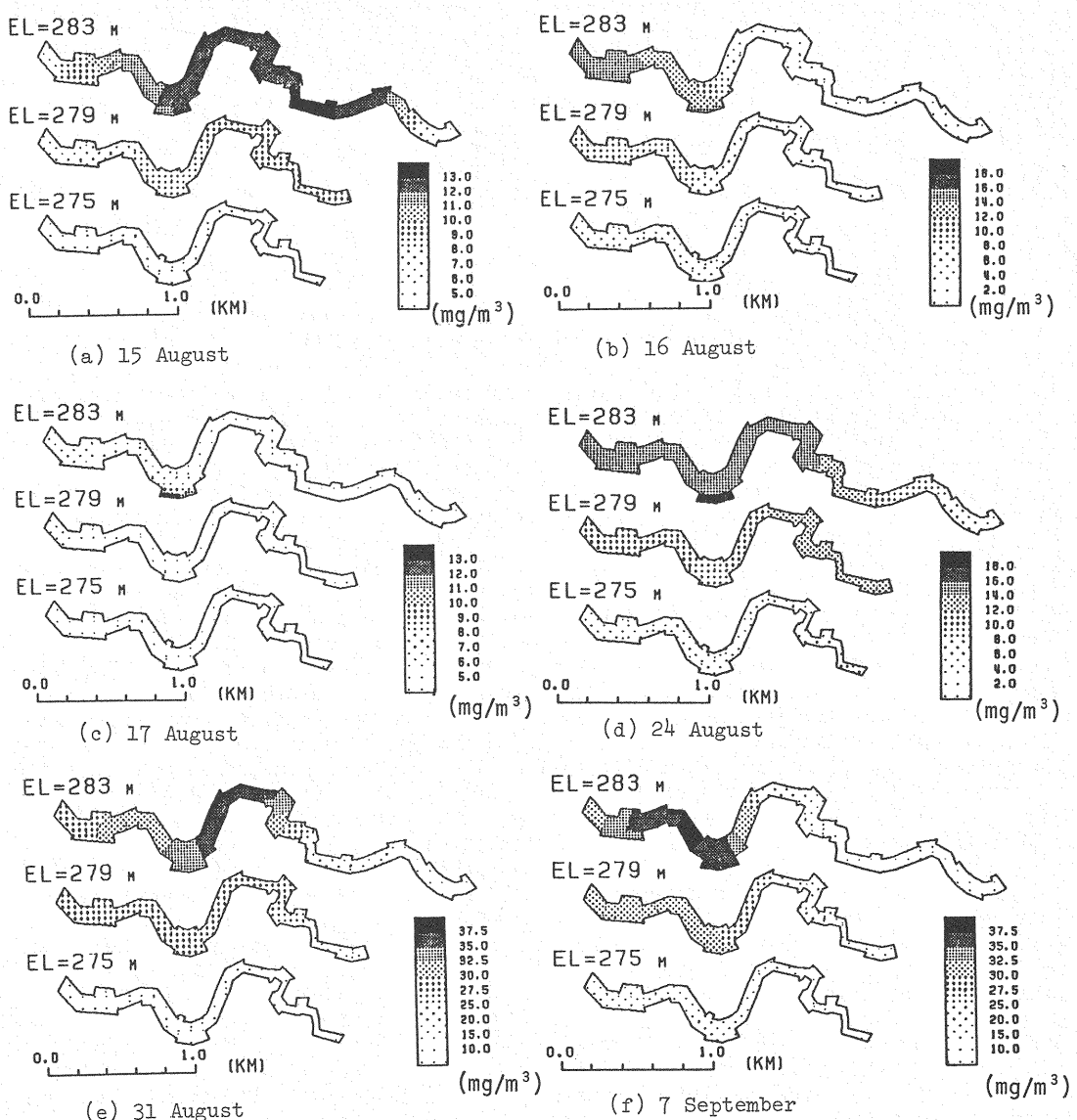

Fig.4 Simulated distributions of chlorophyl-a concentration

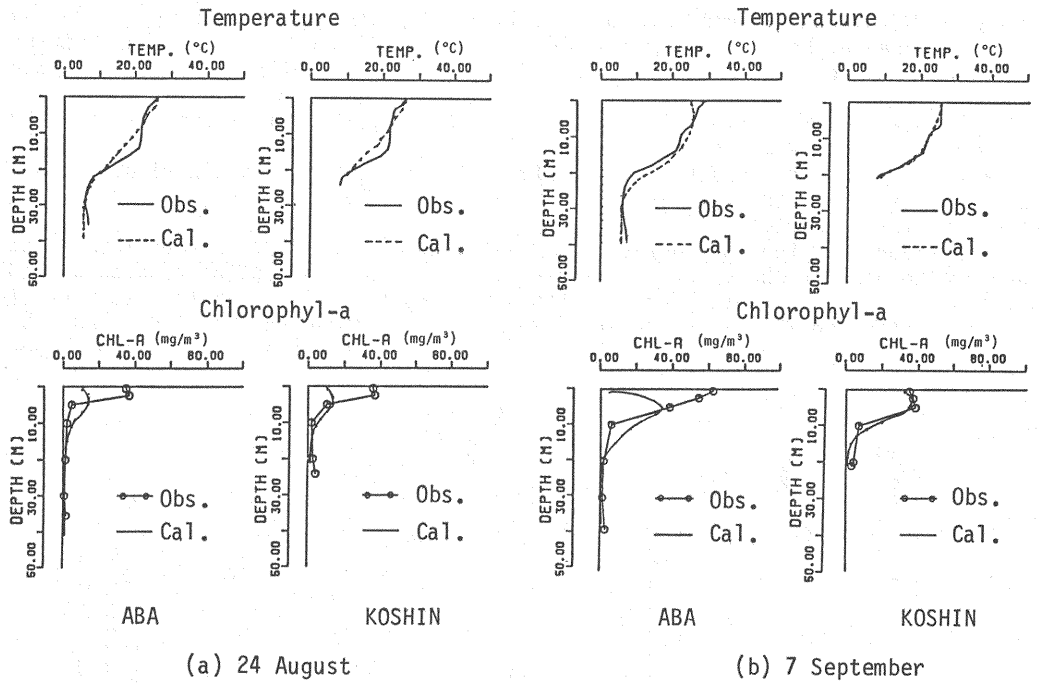

Fig.5 Comparison between simulated values and observed one in terms of water temperature and chlorophyl-a concentration

dam from the results of 24 and 31 August, and their distribution patterns are more evident on 31 August when the flow is very slow.

3) On 16 August, during passing flood, the retention of flow is not found in the surface and upper layers except at the inlets near the plunging point.

Fig.4 indicates the distributions of chlorophyl-a equivalent to the amount of phytoplanktons. It is recognized that the occurring process of phytoplankton blooms is related to the hydraulic characteristics of the flow explained above. After the surface water containing of 15 mg/m^3 chlorophyl-a concentration, located arround the intake at Hatsuse, is discharged with passing flood, the primary production of phytoplanktons becomes gradually active in the surface layer. Consequently, high concentration of 40 mg/m^3 chlorophyl-a will result as shown in Fig.4(f). The occurrence of phytoplankton blooms after a flood passed as simulated in this case study has been often observed in the Muroh reservoir and the others(7).

The phenomena represented here are considered to be originally caused by the large amount of nutrients with the flood. The hydraulic behaviours of the flow and the change of the temperature distribution also contribute a great deal to the phenomena. For example, the area of long retention time after the flood shown in Fig.3 agrees with the area of high chlorophyl-a concentration shown in Fig.4. This result indicates a close relation between the retention time of flow and the growth of phytoplanktons. On the other hand, as seen in Fig.4(a) to (c), a part of chlorophyl-a observed before the flood still remains in the inlet located at the left side of central region of the reservoir during the flood. The staying phytoplanktons increase after the flood and they are transported down- and up-streams in the surface layer by the flow shown in Fig.2(c). These processes produce to the distribution of chlorophyl-a on 24 August shown in Fig.4(d).

High concentration area moves 1.5km downstream for 1 day from 15 to 16 August and 1.0km downstream for 7 days from 31 August to 7 September. The distances are almost equal to the estimated one with the averaged flow velocities of 1.5 and 0.15km/day during the periods, respectively. This result indicates that the movements of high concentration areas are due to the flows.

Finally, the comparative indications of simulated values and observed ones in

terms of the water temperature and the chlorophyl-a concentration are in Fig.5. Regarding the temperature, the simulated values agree almost with the observed ones. On the other hand, comparison between the simulated values of chlorophyl-a near the surface with the observed one are not so satisfactory except for the result at Koshin(center of reservoir) on 7 September. Nevertheless, their profiles are considerably reproduced by the simulation. Uncertain and unknown factors like the inflow condition of nutrients and the ecological change of water quality parameters are not insignificant. Therefore, disagreements between simulated values and observed ones in terms of the chlorophyl-a can be acceptable within a desired degree of data accuracy.

SUMMARY

The numerical study of eutrophication phenomena in a reservoir has been presented. The plane multi-layered model based on the curvilinear orthogonal coordinate system are applied to simulate phytoplankton blooming in the Muroh Reservoir. The validity of the numerical models has been verified successfully. Furthermore, the hydrodynamics of flow, the change of water quality parameters concerning the phytoplankton blooms and their interrelation were discussed. These results are new and useful informations for water quality management in reservoirs.

Finally, the authors would like to thank Naoyuki Fukui, graduate student of Kyoto University, for his sincere assistance, and further Grand-In-Aid for scientific research (general research (c), representative: Naoki Matsuo) financially encourage a part of this study.

REFERENCES

1. Ikeda,S., Y.Inoue and S.Imai : Multispecies of planktons and nutrients model of lake eutrophication, A simulation study in Lake Biwa, State-of-the art in eccological Modelling, Vol.7, PP.501-526, 1978.
2. Iwasa,Y., S.Shiino, N.Matsuo and S.Wakabayashi : Numerical analysis of topographyical feature on reservoir hydraulics, Annuals, Disas. Prev. Res. Inst., No.33B-2, pp.305-321, 1990. (in Japanese)
3. Chapra,S.C., D.Scavia, G.A.Lang and K.H.Reckhow: Models of kinetic resolution, Engineering Approaches for Lake Management, Vol.2 , Butterworth Publishers, Boston, pp.243-339, 1983.
4. Gallerano,F., A.Misiti and R.Ricci : Threedimensional analysis of eutrophication in lakes, Proc. 23rd Cong. IAHR, pp.D107-D114, 1989.
5. Kimmel,B.L., O.T.Lind and L.J.Paulson: Reservoir primary production, Reservoir Limnology, John Wiley & Sons, Inc., U.S.A., pp.133-194, 1990.
6. Matsuo,N., Y.Iwasa, S.Shiino and N.Wakabayashi : Numerical analysis of two-directional multi-layered flow by use of curvilinear orthogonal coordinate system, Proc. of Japanese Conference on Hydraulic Engineering, JSCE, Vol.34, pp.629-634, 1990. (in Japanese)
7. Watanabe,K. : Study of the effect on water quality improvement by means of circulation induced by aeration, Master's thesis of Kyoto University, 1987. (in Japanese)

APPENDIX-NOTATION

The following sysmbols are used in this paper:

a_{z_i} = assimilation rate of carbon in phytoplankton i;

c = concentration of water quality parameters;

C_O = concentration of chemical oxgen demand;

C_{P_i} = concentration of chlorophyl-a in phytoplankton i described in the present paper;

d_i = grazing rate as to phytoplankton i by zooplankton;

D_{ci} = dispersion coefficient of concentration in i direction ($i=x_1, x_2, x_3$);

D_{Ti} = dispersion coefficient of temperature in i direction ($i=x_1, x_2, x_3$);

E_{ij} = coefficient of eddy viscosity in j direction concerning u_1 ($i=x_1, x_2$ and $j=x_1, x_2, x_3$);

f_P, f_C = production rate and decomposition rate of C_O;

g = gravitational acceleration;

$G_{C_{P_i}}$ = primary production term of phytoplankton i;

G_{z_i} = grazing term of zooplankton as to phytoplankton i;

h_1, h_2, h_3 = metric coefficients of distances x_1, x_2 and x_3;

H_T = temperature generation term by radiation;

I_{x_3}, I_O = light intensity at x_3 and at water surface;

$K_{NI}, K_{P_{I_i}}$ = Michaelis constant of N_I, P_I;

$K_{C_{P_i}}$ = saturation constant of grazing as to C_{P_i};

n_i = constant of inhibition due to temperature;

N_I = concentration of inorganic nitrogen;

N_O = concentration of organic nitrogen;

p = pressure;

P_c = ecological production term of water quality parameters;

P_I = concentration of inorganic phosphorus;

P_O = concentration of organic phosphorus;

$R_{C_{P_i}}, R_z$ = death rate of C_{P_i} and Z;

R_{G_i} = maximum production rate of C_{P_i};

R_N, R_P = mineralization rate of nitrogen and phosphorus;

S_c = settling term of water quality parameters;

S_{P_i}, μ_S = space effect coefficient and constant for its calculation;

T = water temperature;

T_{f_i}, I_{S_i} = optimum temperature and light intensity of primary production as to phytoplankton i;

u_1, u_2, u_3 = mean velocity components in x_1-wise, x_2-wise and x_3-wise direction;

w_i = settling velocity of water quality parameter i($i=C_{P_i}, N_O, P_O, C_O$);

Z = concentration of carbon in zooplankton;

α_i = proportion of carbon to chlorophyl-a in phytoplankton i;

β_N, β_P = proportion of nitrogen and phosphorus to chlorophyl-a in phytoplanktons;

γ_N, γ_P = proportion of nitrogen and phosphorus to chlorophyl-a in zooplanktons;

ρ = density of water; and

η, η_O, μ_n = declining coefficients of light intensity in stored waters influenced

(Received November 5, 1991; revised march 26, 1992)